PROPERTIES OF OXIDIZED SILICON AS DETERMINED BY ANGULAR-DEPENDENT X-RAY PHOTOELECTRON SPECTROSCOPY

J.M. HILL, D.G. ROYCE, C.S. FADLEY *, L.F. WAGNER
Department of Chemistry, University of Hawaii, Honolulu, Hawaii 96822, USA

and

F.J. GRUNTHANER
Jet Propulsion Laboratory, Pasadena, California 91103, USA

Received 29 June 1976

Silicon with thermally-grown oxide overlayers in the thickness range 15–89 Å is studied by angular-dependent XPS. Electron attenuation lengths at 1382 eV are found to be 37 ± 4 Å in SiO_2 and 27 ± 6 Å in Si. Single-crystal effects and thin-layer anomalies are also discussed.

1. Introduction

Several prior studies [1–5] have demonstrated the selective surface enhancement that can be achieved in X-ray photoelectron spectroscopy (XPS) by utilizing low – or grazing – electron exit angles. These investigations have also suggested that surface layer thicknesses or electron attenuation lengths can be determined from quantitative analyses of angular-dependent peak intensities [2–5], provided that the effects of surface roughness are adequately allowed for [3–5]. The only prior analysis of such data for a well-defined surface layer was performed by Fraser et al. [2] and dealt with a Cs monolayer on a Mo substrate. Although the experimental data were in good agreement with a macroscopic theoretical model for such phenomena [2], the use of a non-macroscopic surface layer and a substrate with undefined surface profile prevents considering this as a definitive test of the method.

In this letter, we utilize angular-dependent XPS to study highly-polished silicon single crystals with macroscopically-thick, thermally-grown oxide layers. The oxide thicknesses are independently determined by ellipsometry, and the angular distribution (AD) data are analyzed in a self-consistent manner to yield electron attenuation lengths. Oxidized silicon has also been the subject of prior fixed-angle XPS studies which provide certain comparative data [6–8]. An additional type of effect noted in this investigation is fine structure in the angular distributions caused by electron diffraction effects; such phenomena have been observed previously in XPS studies of single-crystal NaCl [9], Au [1,5], and KCl [10]. The influence of such single-crystal effects on theoretical analyses based upon a polycrystalline model is also discussed.

2. Experimental procedure

Oxidized specimens were prepared from single-crystal wafers of p-type, boron-doped silicon with 0.04–0.05 Ω cm resistivity and ⟨100⟩ orientation. These wafers were polished by chemical/mechanical methods [11], pre-oxidized in mixtures of O_2 and H_2O at 850°C to a thickness of ≈1000 Å, stripped in HF to remove all oxide, and finally oxidized to various desired thicknesses at temperatures of 775–900°C in mixtures of dry O_2 and N_2 [12]. All specimen handling

* Alfred P. Sloan Foundation Research Fellow.

after oxide growth, including transfer into the photoelectron spectrometer, was carried out in inert atmospheres of either dry nitrogen or argon. Different specimens from a single preparative sequence were examined by scanning electron microscopy (SEM), ellipsometry, and XPS. The SEM results indicated no significant surface roughness contours for either substrates (after the intermediate HF etch) or final oxidized specimens. At a magnification of 80 000, the only features noted were very faint protrusions of ≈ 100 Å diameter and a mean separation of ≈ 500 Å. The relative heights of these protrusions were estimated to be $\lesssim 50$ Å; more quantitative determinations are presently underway. Oxide film thicknesses were determined ellipsometrically by standard procedures [6,13]. The ellipsometric parameters were: 6328 Å radiation, 45.00° quarter-wave plate orientation, 70.00° incidence angle, and indices of refraction of 1.458 for SiO_2 and $3.884 - 0.023i$ for Si. The four thicknesses studied were found to be $t = 14.5 \pm 0.4$ Å, 37.4 ± 0.5 Å, 63.6 ± 0.5 Å, and 88.6 ± 0.9 Å. As references for absolute XPS peak intensities, additional specimens composed of pure single-crystal Si with approximately a single monolayer of oxide and pure amorphous SiO_2 in the form of optically-smooth quartz were studied.

The photoelectron spectrometer utilized was a Hewlett Packard 5950A specially modified so as to permit computer-controlled specimen rotation in situ at near ultrahigh vacuum conditions of $(2-6) \times 10^{-9}$ torr [3–5]. These pressures are thus considerably lower than the $\approx 10^{-6}$ torr achieved in certain prior XPS studies of Si/SiO_2 [6]. Monochromatized Al Kα radiation was used for excitation, and all measurements were performed at 25–28°C. Specimen rotation was about an axis oriented perpendicular to the plane containing the fixed X-ray incidence – and electron exit – directions. The rotation axis was in the specimen surface and also coincided with a ⟨110⟩ direction. Such rotation varied the polar angle θ of electron emission with respect to the surface, where θ is defined such that 90° corresponds to exit perpendicular to the surface. Peak intensities were determined as a function of θ for all distinguishable core peaks [14] by performing least-squares fits of gaussian functions with smoothly-added constant inelastic tails [15], thereby eliminating any errors caused by the angular-dependent resolution of the spectrometer [16]. The peaks studied and their average kinetic energies were: Si2s (oxide) and Si2s (element) – 1331 eV, Si2p (oxide) and Si2p (element) – 1382 eV, O1s – 950 eV, and C1s – 1197 eV. Carbon was the only impurity noted. Typical C1s relative intensities were very stable with time, and their magnitudes (C1s/Si2p (oxide) $\approx 0.1-0.4$) indicated a contaminant coverage of approximately one monolayer [14]. All absolute peak intensities in this spectrometer are proportional to a smoothly-varying, θ-dependent, instrument response function [3,5] that has normalized values of 1.00 at 90°, 0.47 at 50°, 0.09 at 10°, and zero at 0° [16]. All quantitative analyses were performed with ratios of intensities, thereby canceling such purely instrumental effects. Duplicate specimens of each oxide thickness were studied.

3. Results and discussion

Of particular interest is the intensity ratio of the chemically-shifted oxide – and element – peaks for Si2s and Si2p core levels (R(ox/el)), as such angular-dependent data are amenable to rather direct theoretical analysis [3]. Typical Si2p spectra for a specimen with a 14.5 Å oxide layer are shown in fig. 1 at $\theta = 80°$, 20°, and 3°. A purely instrumental increase in linewidth occurs as θ is varied in either direction away

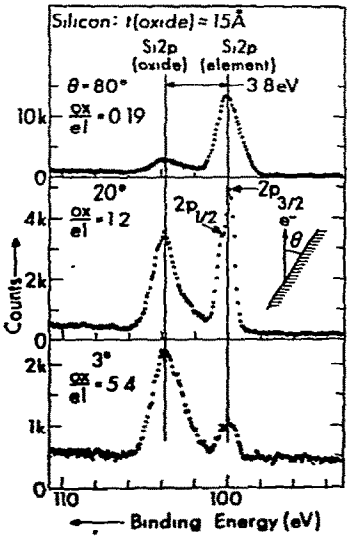

Fig. 1. Si2p spectra at three different electron exit angles for a silicon specimen with a 14.5 Å thick oxide overlayer.

from approximately 30° [16]. There is a complete inversion in the oxide/element ratio, with the oxide relative intensity being increased by a factor of 28 between 80° and 3°. Such intensity ratios were determined for both Si2s and Si2p spectra over the angle range $5° \lesssim \theta \lesssim 90°$. The 2p ratio data are summarized by the points and solid curves in fig. 2. (The method of plotting utilized is justified below.) The Si2s spectra, although not as well resolved into oxide and element components as those of Si2p, gave ratio data in excellent agreement with fig. 2 [14].

Analyses of spectra such as those in fig. 1 for all four thicknesses reveal two types of peculiarities in the specimens with 14.5 Å oxide layer: (1) For these specimens, there is noticeable asymmetry of the oxide peak such that intensity is enhanced towards lower binding energies. To a certain degree, this effect was also noted in the data for the 37.4 Å specimens; however, it was less pronounced. Such asymmetries could be due to a certain fraction of silicon atoms being present in oxidation states lower than SiO_2. (2) The chemical shift between the primary oxide peak and the element peak is significantly less for the 14.5 Å specimens, with the various values being 3.8 ± 0.1 eV for 14.5 Å, 4.5 ± 0.1 eV for 37.4 Å, 4.4 ± 0.1 eV for 63.6 Å, and 4.3 ± 0.1 eV for 88.6 Å. A predominance of lower oxidation states in the 14.5 Å layer could also explain this result. Although surface charging in the oxide layer also could produce both of these effects [14], it was ruled out as the primary cause because peak positions and shapes were stable during exposure to a low-energy electron flood gun with energies of up to 2 eV and currents of up to 0.1 mA, and also because peak positions were constant with angle (and thus also with mean emission depth). These observations are consistent with prior studies suggesting either a non-stoichiometric character for oxide layers thinner than ≈20–40 Å [6,8], or other shift-inducing effects more specifically associated with the element/oxide interface [7]. Thus, the 37.4 Å, 63.6 Å and 88.6 Å specimens are the most unambiguously representative of well-characterized SiO_2 overlayers, although the 37.4 Å oxide layers may also deviate slightly from this description.

A further effect that must be considered in analyzing such XPS data is the presence of fine structure in the angular distributions caused by the single-crystal character of the specimens. Such effects are clearly present in the Si2p (element) angular distributions of fig. 3, which are shown for four different oxide layer thicknesses: ≈3 Å, 14.5 Å, 37.4 Å, and 88.6 Å. The 3 Å specimen was prepared by subjecting a Si wafer to an HF etch and subsequent rinses with distilled water and ethanol immediately before insertion into the spectrometer; the thickness was estimated from O1s/Si2p (element) ratios, and corresponds to approximately a monolayer of oxide. The fine structure is

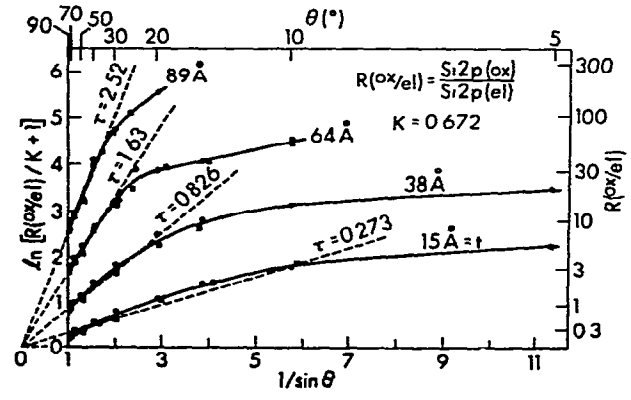

Fig. 2. Angular-dependent Si2p(oxide)/Si2p(element) ratio data for silicon specimens with four different oxide layer thicknesses. Experimental data is shown as points and solid curves, with the two different symbols representing separate specimens. The form of the plot is that of eq. (4) with K = 0.672. The dotted lines are least-squares fits of eq. (1) to the data for each thickness with K = 0.672.

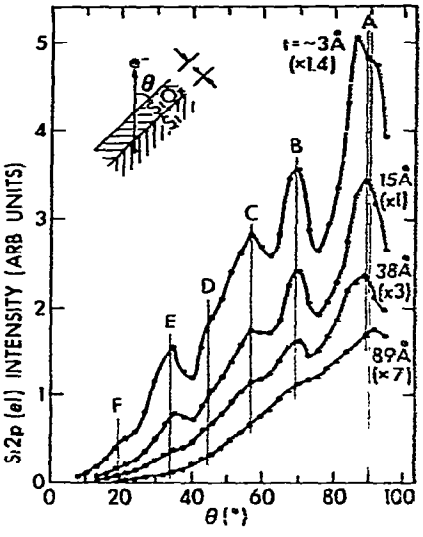

Fig. 3. Si2p(element) angular distributions for four different oxide thicknesses. Features A–E are due to electron diffraction effects in the single crystal substrate.

most pronounced for the thinnest oxide layers, where it consists of maxima and minima with relative amplitudes of approximately ±20% as measured with respect to a smooth-curve average, and it is progressively attenuated as the thickness increases. The same basic features A–F are found in all curves. The origins of these effects are closely related to the Kikuchi bands observed in low energy electron diffraction studies [1,5,9,10,17]. Peak A corresponds to electron emission along a ⟨100⟩ direction and peak E to emission along a ⟨111⟩ direction. By contrast, corresponding angular distributions from O1s and Si2p (oxide) exhibited no fine structure whatsoever, thus strongly indicating an amorphous oxide layer that acts to smear out substrate single-crystal effects by various quasi-elastic scattering processes. It is significant that the relative amplitudes of features A–F decrease by only ≈4% for an oxide thickness change from approximately 3 to 15 Å. This indicates that such scattering events are relatively weak in distorting angular distributions over distances of the order of the inelastic scattering attenuation length Λ_{ox}, but they may not be completely negligible, as has been assumed previously [2,3,5].

Such single-crystal effects on Si2p (element) intensities will thus introduce similar fine structure with maximum amplitudes of ≈±20% in the ratio R(ox/el). Such phenomena could have been present in prior studies of Si/SiO_2 by fixed-angle XPS [6,7], but have not been discussed previously. If this is the only effect associated with single-crystal character, and if it is further noted that surface-layer/substrate relative intensities often extend over an order of magnitude or more in range (cf. fig. 2), it might still be expected that an analysis of angular-dependent ratio data in terms of a polycrystalline model would yield a reasonably good average description in terms of macroscopic specimen properties, and it is this procedure that is attempted here. However, it is also possible that a smooth-curve average over such single-crystal structure may not be the same as the corresponding curve from a polycrystalline – or amorphous – substrate [5,18]. If this is true, the specimens with thinnest oxide layers, specifically, 14.5 Å and, to a lesser degree, 37.4 Å, might again be expected to exhibit somewhat more complex behavior.

4. Analysis of angular distribution data

A polycrystalline, macroscopic model for describing ratio data such as that in fig. 2 has been discussed previously [2,3,5]. Because the peaks involved in R(ox/el) are very close in kinetic energy and also have a common subshell of origin, simplifying cancellations of three common factors occur in the ratio: (1) the instrument response function, (2) the attenuation due to inelastic scattering in any surface contaminant layer, and (3) the differential photoelectric cross section, which is assumed to change negligibly from oxide to element. The final expression for the θ-dependent ratio is thus [3,5]:

$$R(\mathrm{ox/el}) = K[\exp(\tau/\sin\theta) - 1] \,, \tag{1}$$

in which K is a constant given by

$$K = \rho_{ox}^{Si}\Lambda_{ox}/\rho_{el}^{Si}\Lambda_{el} \tag{2}$$

and τ is an effective oxide layer thickness

$$\tau = t/\Lambda_{ox} \,. \tag{3}$$

Here, ρ_{ox}^{Si} is the Si number density in the oxide, ρ_{el}^{Si} is the Si number density in the element, Λ_{ox} is the electron attenuation length in the oxide, and Λ_{el} is the electron attenuation length in the element. If K is assumed known, eq. (1) is easily converted to a form involving a linear relationship between experimentally-derivable quantities:

$$\ln[R(\mathrm{ox/el})/K + 1] = \tau/\sin\theta \,. \tag{4}$$

It is this form that has been used in plotting the data in fig. 2, together with an empirical value for K of 0.672 determined as indicated below. Note the requirement imposed by this equation that all theoretical lines pass through the origin.

It is also a straightforward matter to show that, at a given angle, the ratio of corresponding silicon core-peak intensities from infinitely-thick oxide – and element – specimens is equal to the constant K [2,3,5,6]. That is,

$$K = N_\infty(\mathrm{ox})/N_\infty(\mathrm{el}) \equiv R_\infty(\mathrm{ox/el}) \,, \tag{5}$$

where N_∞ indicates an absolute peak intensity from an infinitely-thick specimen. Eq. (5) requires for its validity that inelastic attenuation in any contaminant surface layers present either be very small or at least approximately equal for both types of specimens. C1s

and O1s relative intensities showed this to be the case in the present study, and such absolute intensity ratios were thus used to derive an experimental K of 0.672 ± 0.050. This value corresponds reasonably well with an estimate made by using the known densities for Si and various forms of SiO_2 and further assuming that $\Lambda_{ox} \approx \Lambda_{el}$, as suggested by a previous fixed-angle XPS study [6]. This yielded a range of values for K from 0.441 to 0.543, depending upon the type of SiO_2 crystal structure assumed, with the average being 0.492.

Eqs. (1) and (4) were then utilized to analyze the R(ox/el) data in a self-consistent manner. The R(ox/el) values were plotted as in fig. 2 with $K = 0.672$, and it was noted that, over a limited range of angles extending downward from 90°, the data for the 37.4 Å, 63.6 Å, and 88.6 Å oxide layer thicknesses followed very closely a linear relationship such as that predicted by eq. (4). The lower boundaries for these ranges are approximately 30° for 37.4 Å, and 40° for both 63.6 Å and 88.6 Å. For θ values below these limits, systematic deviations from linearity occur for these thicknesses in such a direction that the experimental R(ox/el) is below that predicted by eq. (4) (cf. fig. 2), and these results thus indicate a reduced surface sensitivity relative to simple theory. By contrast, the 14.5 Å data exhibit more significant curvature in such a plot (cf. fig. 2), and can only be considered approximately linear down to $\theta \approx 30°$. The low-θ deviations and associated curvature noted for all specimens could be caused by several effects:

(1) Residual surface roughness – Model calculations for periodic surface profiles [3,5] indicate that deviations of the magnitudes observed could be produced by roughness with an amplitude-to-wavelength ratio of approximately 0.1–0.2, and it is possible on the basis of the scanning electron micrographs for surface roughness of that degree to have been present.

(2) Electron refraction at the surface during electron emission – Simple step-potential calculations using a reasonable range of inner potentials (5–20 eV) [5,14] indicate that refraction effects should not become important for the ≈1.5 keV electrons in XPS until $\theta \lesssim 10°$.

(3) A diffuse boundary between oxide and element – For a linear-gradient transition region centered at depth t, theoretical estimates of these effects are found to be in the proper direction but too small in magnitude for a realistic range of transition-region thicknesses ($\lesssim t$).

(4) Elastic electron scattering – For electron detection at low θ, elastic scattering could decrease the average attenuation due to inelastic scattering for emission from greater depths within the specimen by causing electrons that have had reasonably large θ values during much of their escape to be scattered to low θ near the surface. No quantitative estimates of this effect were made. Thus, residual roughness emerges as the most likely primary source of the low-angle deviations, although several effects may be working in concert. The low-angle data was thus disregarded in the remainder of the analysis.

Eq. (1) was then least-squares fit to the data for the selected ranges in two different ways to check for self-consistency. These results are summarized in table 1 and the fitting methods were:

(1) The data for each thickness as a function of θ were fit separately, with both K and τ as adjustable parameters: the results for the two thickest oxide layers are in very good agreement with one another, with K values that are very close and an average K of 0.695 that is quite near to the experimental K of 0.672. The resultant Λ_{ox} values obtained for these two thicknesses are also within 13% of one another, and yield an average of 37.6 Å. The least-squares parameters obtained for the 37.4 Å oxide layer are both somewhat smaller than those for 63.6 Å and 88.6 Å, although there is reasonable agreement, particularly for Λ_{ox}. By contrast, the 14.5 Å values for

Table 1
Summary of parameters obtained from least-squares analyses of angular-dependent Si2p(oxide)/Si2p(element) ratios according to eqs. (1) and (4). Oxide layer thicknesses t were determined ellipsometrically, and Λ_{ox} values were calculated from eq. (3). The mean electron kinetic energy is 1382 eV

t (Å)	Linear date range	K [a]	Λ_{ox} (Å) [a]	Λ_{ox} (Å) [b] ($K = 0.672$)
88.6	40°–90°	0.686	35.3	35.1
63.6	40°–90°	0.703	39.8	39.1
37.4	40°–90°	0.353	31.3	45.3
14.5	30°–90°	(0.072)	(12.4)	53.1

a) Two-parameter fit of eq. (1) over linear data range.
b) One-parameter fit of eq. (1) over linear data range, with K fixed at experimental value.

both K and Λ_{ox} are much smaller, thereby further confirming the more complex behavior associated with this thickness, as perhaps caused by altered stoichiometry or more pronounced single-crystal effects. (2) The data for each thickness were fit separately, with K equal to the experimental value of 0.672: this gives Λ_{ox} values for the two thickest oxide layers that are very close to those in the prior two-parameter fit. For the two thinnest oxide layers, attenuation lengths $\approx$20–40% larger are found, but there is still reasonably good agreement. Thus, with an independently determined K value, the angular-dependent data for all four thicknesses are best described by a fairly narrow range of attenuation lengths from 35 to 53 Å.

As might be expected, either one-parameter – or two-parameter – least-squares fits are found to yield values for $\tau = t/\Lambda_{ox}$ (a parameter that controls the large changes occurring in R(ox/el) with θ via an exponential function) that span a significantly narrower range than the corresponding values for K (a parameter that is simply a scale factor). This is particularly true for the two thickest oxide layers, for which an arbitrary 20% change in K produces only a 6–8% change in the associated least-squares values of τ (or Λ_{ox}). The separate determination of K from eq. (5) thus should significantly improve the overall accuracy of such least-squares analyses of ratio angular distribution data.

On the basis of chemical-shift magnitudes, symmetric peak shapes, decreased single-crystal effects, and observed conformity to the theoretical model, the two thickest oxide layers are thus expected to be most reliably indicative of a macroscopic Si/SiO_2 geometry, and their average behavior is used to determine a final best value for Λ_{ox} of 37 ± 4 Å. It is then possible to determine the attenuation length in elemental silicon from eq. (2), yielding Λ_{el} = 27 ± 6 Å; the slightly larger uncertainty arises because of the range of densities possible for the oxide layer. Attenuation length values obtained from a similar analysis of Si2s (oxide)/Si2s (element) ratios are furthermore in complete agreement with these numbers [14]. Our final Λ_{ox} value is thus significantly higher than, but in approximate agreement with, the 27 ± 2 Å reported previously by Flitsch and Raider [6] and determined from fixed-angle XPS measurements of R(ox/el) at various oxide thicknesses between 20 Å and 120 Å; our Λ_{el} value is, on the other hand, in good agreement with their 26 ± 2 Å.

5. Concluding remarks

Angular-dependent XPS has been applied to the Si/SiO_2 system as an example of a relatively well-defined macroscopic overlayer/substrate geometry. Certain anomalies are noted in chemical shifts and peak shapes for oxide thicknesses below $\approx$40 Å. Analysis of relative-intensity angular distribution data yields self-consistent electron attenuation lengths with accuracies that are comparable to fixed-angle overlayer methods, and suggests the general utility of this procedure. However, unambiguous interpretation of such data requires that surfaces be carefully prepared to insure near planarity, that the constant K multiplying the basic theoretical expression be determined independently, that preliminary tests of the data against expected theoretical forms be made in order to eliminate low-angle regions in which several complicating effects can occur, and that the data analysis be carried out in more than one way to check for self-consistency. The use of single-crystal substrates also introduces significant fine structure in the angular distributions, but, for the Si/SiO_2 system, analysis in terms of a macroscopic polycrystalline model appears to average over these effects in a meaningful way, particularly for oxide layers with thicknesses $\gtrsim$ 40 Å.

Acknowledgement

We gratefully acknowledge the support of the National Science Foundation (Grants GP38640X and MPS75-05055), the Alfred P. Sloan Foundation, and the National Aeronautics and Space Administration.

References

[1] C.S. Fadley and S.A.L. Bergström, Phys. Letters 35A (1971) 375; in: Electron spectroscopy, ed. D.A. Shirley (North-Holland, Amsterdam, 1972) p. 233.
[2] W.A. Fraser, J.V. Florio, W.N. Delgass and W.D. Robertson, Surface Sci. 36 (1973) 661.
[3] C.S. Fadley, R.J. Baird, W. Siekhaus, T. Novakov and S.A.L. Bergström, J. Electron Spectry. 4 (1974) 93; C.S. Fadley, J. Electron Spectry. 5 (1974) 725.
[4] R.J. Baird, C.S. Fadley, S.K. Kawamoto and M. Mehta, Chem. Phys. Letters 34 (1975) 49.
[5] C.S. Fadley, Comments in Faraday Discussion No. 60 (1975); in: Progress in solid state chemistry, Vol. 11,

Part 3, eds. G.A. Samorjai and J.O. McCaldin (Pergamon Press, London, 1976), to be published.
[6] R. Flitsch and S.I. Raider, J. Vacuum Sci. Technol. 12 (1975) 305;
S.I. Raider, R. Flitsch and M.J. Palmer, J. Electrochem. Soc. 122 (1975) 413;
S.I. Raider and R. Flitsch, J. Vacuum Sci. Technol. 13 (1976) 58.
[7] G. Hollinger, Y. Jugnet, P. Pertosa and Tran Minh Duc, Chem. Phys. Letters 36 (1975) 441.
[8] F.J. Grunthaner, to be published.
[9] K. Siegbahn, U. Gelius, H. Siegbahn and E. Olsen, Phys. Letters 32A (1970) 221; Physica Scripta 1 (1970) 272.
[10] J. Brunner and H. Zogg, unpublished results;
H. Zogg, Ph.D. Thesis, E.T H., Zurich (1974).
[11] P. Rai-Choudhury, J. Electrochem. Soc. 118 (1971) 1183.
[12] J. Maserjian and G.P. Peterson, Appl. Phys. Letters 25 (1974) 50.
[13] R.J. Archer and G.W. Gobelli, J. Phys. Chem. Solids 26 (1965) 343;
Y.S. Vandermeulen, J. Electrochem. Soc. 119 (1972) 530.
[14] J.M. Hill, M.S. Thesis, University of Hawaii, Honolulu (1975).
[15] C.S. Fadley, Ph.D. Thesis, University of California, Berkeley (1970).
[16] R.J. Baird and C.S. Fadley, paper presented at the Northwest Regional Meeting of the American Chemical Society, Honolulu, Hawaii, June (1975); to be published.
[17] R.J. Baird, C.S. Fadley and L.F. Wagner, to be published.
[18] D.P. Woodruff, Faraday Discussion No. 60 (1976), to be published.